The Multispectral Microscopic Imager: Integrating Microimaging with Spectroscopy for the In-Situ Exploration of the Moon. J. I. Nuñez[1], J. D. Farmer[1], R. G. Sellar[2], and C. C. Allen[3], [1]School of Earth and Space Exploration, Arizona State University, Tempe, AZ 85287. (jorge.nunez@asu.edu and jack.farmer@asu.edu), [2]Jet Propulsion Laboratory, California Institute of Technology, Pasadena, CA 91109. (glenn.sellar@jpl.nasa.gov), [3]NASA Johnson Space Center, Houston, TX 77058. (carlton.c.allen@nasa.gov).

Introduction: To maximize the scientific return, future robotic and human missions to the Moon will need to have *in-situ* capabilities to enable the selection of the highest value samples for returning to Earth, or a lunar base for analysis. In order to accomplish this task efficiently, samples will need to be characterized using a suite of robotic instruments that can provide crucial information about elemental composition, mineralogy, volatiles and ices. Such spatially-correlated data sets, which place mineralogy into a microtextural context, are considered crucial for correct petrogenetic interpretations. .

Combining microscopic imaging with visible– near-infrared reflectance spectroscopy, provides a powerful *in-situ* approach for obtaining mineralogy within a microtextural context. The approach is non-destructive and requires minimal mechanical sample preparation. This approach provides data sets that are comparable to what geologists routinely acquire in the field, using a hand lens and in the lab using thin section petrography, and provide essential information for interpreting the primary formational processes in rocks and soils as well as the effects of secondary (diagenetic) alteration processes. Such obervations lay a foundation for inferring geologic histories and provide "ground truth" for similar instruments on orbiting satellites; they support astronaut EVA activities and provide basic information about the physical properties of soils required for assessing associated health risks, and are basic tools in the exploration for *in-situ* resources to support human exploration of the Moon.

Instrument: The Multispectral Microscopic Imager (MMI) generates multispectral, microscale reflectance images of geological samples, where each pixel consists of a spectrum ranging from 463 nm to 1750 nm [1], [2]. This spectral range enables the discrimination of a wide variety of rock-forming minerals, especially Fe-bearing phases, within a microtextural framework.

Investigation of Apollo Samples: To assess the value of the MMI as a tool for lunar exploration, we transported a field-portable, tripod-mounted version of the MMI to the Lunar Experiment Laboratory at NASA's Johnson Space Center [1], [3], [4]. We used the instrument to image 18 lunar rocks and four soils, selected from a reference suite that spanned the full compositional range of the Apollo collection.

Figures 1 and 2 show natural-color (A) and false-color composite images (B) obtained with the MMI, false-color RGB composite images, where each color depicts the ratio of two MMI bands (C), and mineral maps (D) based on spectral end-members (E) created using the analytical software, ENVI. In each Figure, images labeled C are based on band ratios similar to those used with the Clementine mission's UV-VIS camera, which reveals important mineralogical features of the lunar surface . The red channel is the ratio 741/463-nm (analogous to UV-VIS' 750/415-nm), which is sensitive to the presence of plagioclase, or mature regolith (characterized by an increased reflectance slope due to the prescence of nanophase Fe^0 and associated "agglutinates" produced by space weathering processes [5]). The green channel is the ratio 741/970-nm (analogous to UV-VIS' 750/950-nm), which reflects the presence of Fe^{2+} in minerals and glasses [6]. The blue channel is the ratio 463/741-nm (analogous to UV-VIS' 415/750-nm), which correlates positively with the prescence of opaques (e.g. ilmenite) or immature regolith (characterized by the lower abundance of agglutinates and nanophase Fe^0 [7]).

The MMI composite images faithfully resolve the microtextural features of samples, while the application of spectral end-member mapping and band ratios faithfully reveals the distribution of Fe-bearing mineral phases (olivine, pyroxene and magnetite), along with plagioclase feldspars within samples, over a broad range of lithologies and grain sizes (Figures 1 & 2). The MMI composite images and spectra also revealed the presence of ilmenite, glasses, and, where present, the effects of space weathering and secondary mineral phases in samples (Figures 1 & 2).

Our MMI-based petrogenetic interpretations compare favorably with thin section descriptions published in the literature, and reveal the value of MMI images for astronaut and rover-based exploration of the Moon.

References: [1] Sellar R. G. et al. (2008) *Joint Ann. Meet. LEAG-ICEUM-SRR*, Abstract #4075. [2] Nuñez J. I. et al. (2009) *LPSC XL*, Abstract #1830. [3] Allen C. C. et al. (2009) *2nd Lunar Science Forum*. [4] Nuñez J. I. et al. (2009) *2nd Lunar Science Forum*. [5] Taylor L. A. et al. (2001) *JGR* 106, 27,985-27,999. [6] Burns R. G. et al. (1982) *Mineral. App. Cryst. Field Theory*, 2nd Ed, 551pp, Cambridge Univ. Press, NY. [7] Charette M. P. et al. (2001) *JGR* 79, 1,605-1,613.

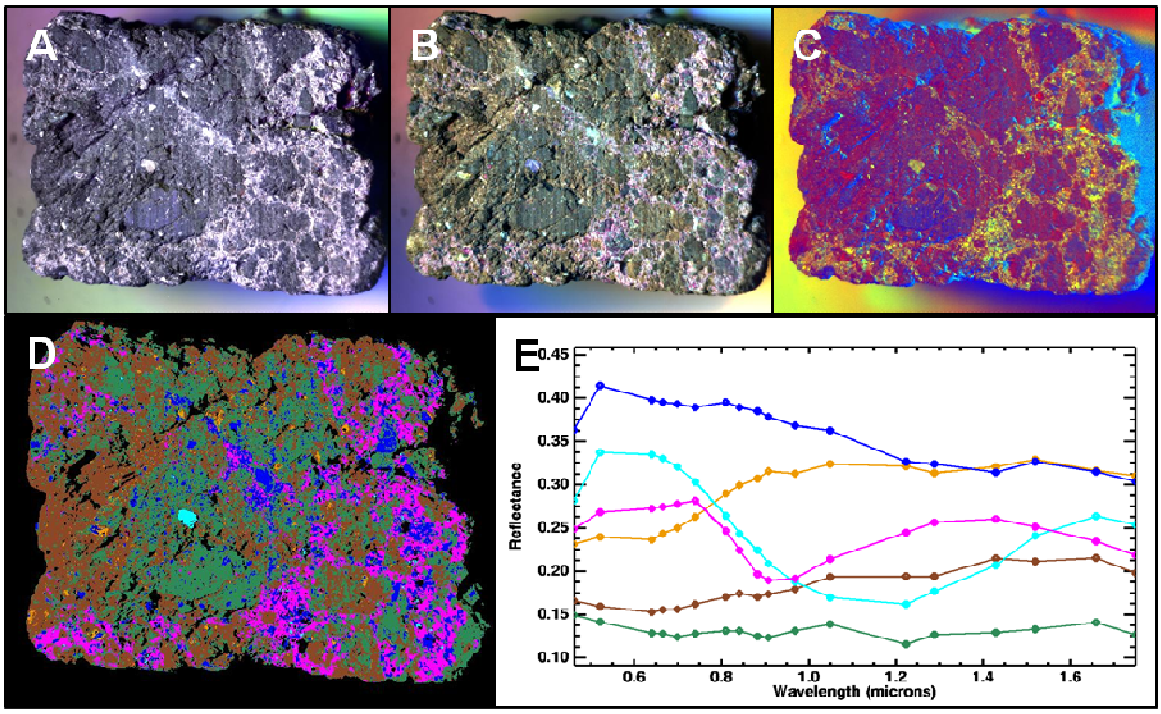

Figure 1. Multispectral images (A & B), RGB composite using MMI band ratios (C), corresponding color mineral map (D) and spectra (E) of Apollo sample 14321,88. Field-of-view: 40 mm x 32 mm (62.5 µm/pixel). Figures A & B are 2% histogram stretched. Figure 1A: R = 641 nm; G = 522 nm; B = 463 nm. Figure 1B: R = 1430 nm; G = 970 nm; B = 522 nm. Figure 1C: R = 741/463; G = 741/970; B = 463/741. Light blue in C correlates with shadow effects. Figure 1D: Color mineral map based on spectral end-members (figure 1E).

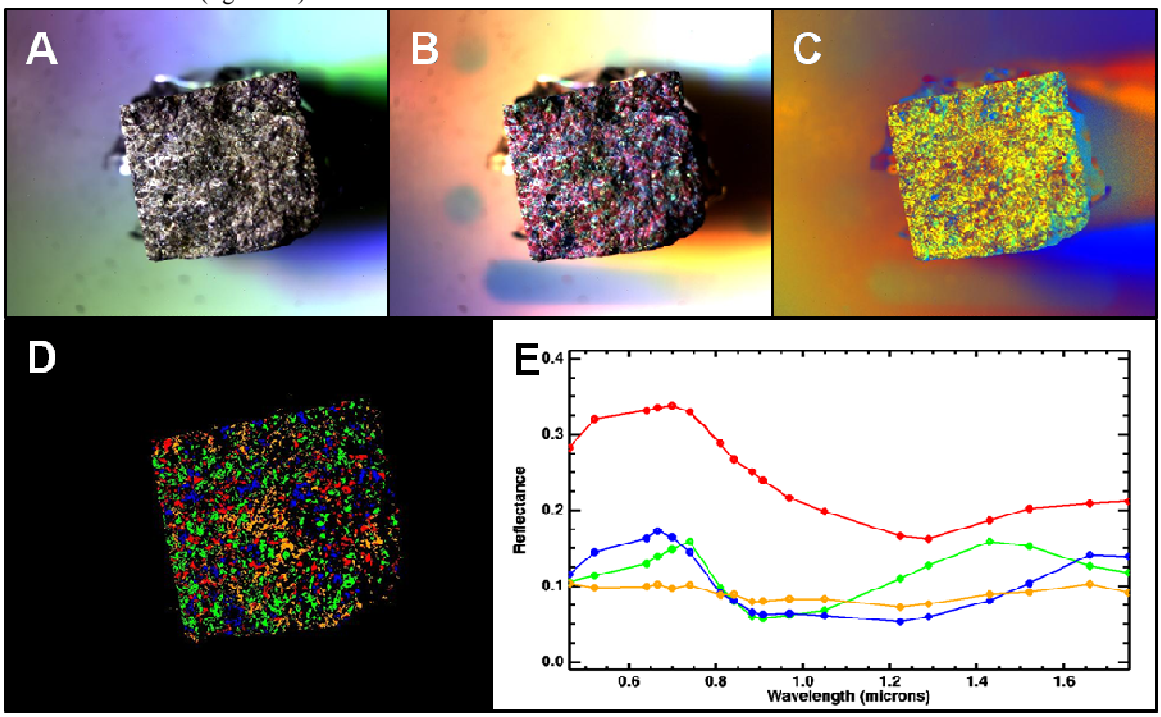

Figure 2. Multispectral images (A & B), RGB composite using MMI band ratios (C), corresponding color mineral map (D) and spectra (E) of Apollo sample 15555,62. Field-of-view: 40 mm x 32 mm (62.5 µm/pixel). Figures A & B are 2% histogram stretched. Figure 2A: R = 641 nm; G = 522 nm; B = 463 nm. Figure 2B: R = 1430 nm; G = 970 nm; B = 522 nm. Figure 2C: R = 741/463; G = 741/970; B = 463/741. Light blue in C correlates with shadow effects. Figure 2D: Color mineral map based on spectral end-members (figure 2E).